

MOL #48900

Title page

The Role of Human Nucleoside Transporters in Uptake of 3'-Deoxy-3'-Fluorothymidine

Robert J. Paproski, Amy M. L. Ng, Sylvia Y. M. Yao, Kathryn Graham, James D. Young, and Carol E.

Cass

Departments of Oncology (R.J.P., K.G., C.E.C) and Physiology (A.M.L.N., S.Y.M.Y., J.D.Y.), University of Alberta, and the Cross Cancer Institute (R.J.P., K.G., C.E.C), Edmonton, Alberta, Canada

MOL #48900

Running title page

Running title: FLT Uptake by Nucleoside Transporters

Address correspondence to: Dr. Carol E. Cass, Department of Oncology, University of Alberta, Cross Cancer Institute, 11560 University Ave., Edmonton, Alberta, Canada T6G 1Z2. Telephone number: (780) 432-8763, Fax number: (780) 432-8886, E-mail: carol.cass@cancerboard.ab.ca

Number of text pages: 28

Number of tables: 3

Number of figures: 7

Number of references: 39

Number of words in Abstract: 243

Number of words in Introduction: 627

Number of words in Discussion: 1390

Abbreviations: PET, positron emission tomography; FLT, 3'-deoxy-3'-fluorothymidine; TK1, thymidine kinase 1; hNT, human nucleoside transporter; hENT, human equilibrative nucleoside transporters; hCNT, human concentrative nucleoside transporters; NBMPR, nitrobenzylmercaptapurine ribonucleoside; NMDG, N-methyl-D-glucamine; CMM, complete minimal medium; GAPDH, glyceraldehyde-3-phosphate dehydrogenase; FTH-SAENTA, 5-S-{2-(1-[(fluorescein-5-yl)thioureido]hexanamido)ethyl}-6-N-(4-nitrobenzyl)-5-thioadenosine.

MOL #48900

ABSTRACT

3'-Deoxy-3'-fluorothymidine (FLT) is a positron emission tomography (PET) tracer used to identify proliferating tumor cells. The purpose of this study was to characterize FLT transport by each human nucleoside transporter (hNT) and to determine the role of hNTs for FLT uptake in various human cancer cell lines. FLT binding to hNTs was monitored by the inhibitory effects of FLT on ^3H -uridine uptake in yeast cells producing recombinant hNT proteins. hCNT1 displayed the lowest FLT K_i value for inhibition of ^3H -uridine uptake, followed by hCNT3, hENT2, hENT1, and hCNT2. ^3H -FLT was efficiently transported in *Xenopus laevis* oocytes individually producing hENT1, hENT2, hCNT1 or hCNT3. ^3H -FLT uptake in MCF-7, A549, U251, A498, MIA PaCa-2, and Capan-2 cells was inhibited at least 50% by the hENT1 inhibitor nitrobenzylmercaptapurine ribonucleoside (NBMPR). Using real-time PCR, hENT1 and hENT2 had the most abundant hNT transcripts in all cell lines. Cell lines also underwent (i) ^3H -NBMPR equilibrium binding assays with or without 5-S-{2-(1-[(fluorescein-5-yl)thioureido]hexanamido)ethyl}-6-N-(4-nitrobenzyl)-5-thioadenosine (FTH-SAENTA), a membrane impermeable NBMPR analog, to determine plasma membrane hENT1 levels, and (ii) dose-response NBMPR inhibition of ^3H -FLT uptake. MCF-7, A549, and Capan-2 cells displayed NBMPR IC_{50} values that were smaller or equal to NBMPR K_d values, suggesting that 50% inhibition of hENT1 reduced ^3H -FLT uptake by at least 50%. A strong correlation between extracellular NBMPR binding sites/cell and ^3H -FLT uptake was observed for all cell lines except MIA PaCa-2. These data suggest that plasma membrane hNTs (especially hENT1) are important determinants of cellular FLT uptake.

MOL #48900

Positron emission tomography (PET) is a useful imaging modality that allows visualization and quantification of molecular markers or processes in tissues. The thymidine analog 3'-deoxy-3'-fluorothymidine (FLT) is considered an indirect proliferation-indicating PET imaging agent because, although it is not incorporated into DNA, its intracellular accumulation correlates well with proliferating cells (Toyohara et al., 2002). Increased FLT accumulation in proliferating cells is believed to be due to a proliferation-dependent increase in thymidine kinase 1 (TK1) activity, leading to increased intracellular phosphorylation and 'trapping' of FLT (Barthel et al., 2005; Grierson et al., 2004; Rasey et al., 2002). However, FLT must cross plasma membranes before it can interact with TK1 and human nucleoside transporters (hNTs) are thought to be involved in this process since FLT uptake in HL-60 cells was significantly reduced by inhibiting human equilibrative nucleoside transporter 1 (hENT1) (Kong et al., 1992).

hNTs are involved in the cellular uptake of physiological nucleosides, nucleoside analogs and in some instances nucleobases (Kong et al., 2004). Extracellular adenosine concentrations, which affect various cardiovascular and neurological processes, are influenced by hNTs (Latini and Pedata, 2001; Shryock and Belardinelli, 1997). Many clinical antineoplastic and antiviral nucleoside analogs gain intracellular access by hNT-mediated transport across plasma membranes (Mackey et al., 1998; Pastor-Anglada et al., 1998).

There are two different families of hNTs: the hENTs (also known as the SLC29 family) and the concentrative nucleoside transporters (hCNTs, also known as the SLC28 family). hENTs mediate bidirectional transport of nucleosides across biological membranes and are found in most tissues in the body. The four hENT family members are hENT1/2/3/4 (Baldwin et al., 2005; Barnes et al., 2006; Griffiths et al., 1997a; Griffiths et al., 1997b). hENT1 appears to be ubiquitously distributed in cells and tissues and has broad permeant selectivity, transporting a structurally diverse array of natural and synthetic nucleosides. NBMPR selectively inhibits hENT1 at nanomolar concentrations and has been used to functionally distinguish hENT1 from other hNTs (Griffiths et al., 1997a). hENT2 is also broadly selective, transporting natural and some synthetic nucleosides as well as some nucleobases. hENT3 is a pH-

MOL #48900

dependent low-affinity transporter of broad nucleoside selectivity with a N-terminal dileucine motif that targets the transporter toward intracellular membranes that co-localize with lysosomal markers (Baldwin et al., 2005). hENT4, found predominantly in the heart and brain, displays pH-dependent adenosine-selective transport (Barnes et al., 2006).

hCNTs couple the transport of nucleosides and sodium or, in the case of hCNT3, protons down their electrochemical gradients to concentrate nucleosides within cells. The three hCNT family members are hCNT1/2/3 (Ritzel et al., 2001; Ritzel et al., 1997; Wang et al., 1997). hCNT1 is pyrimidine nucleoside-selective, transporting uridine, cytidine, and thymidine most efficiently (Ritzel et al., 1997). hCNT2 is purine nucleoside-selective and efficiently transports adenosine, guanosine, and inosine, although it also transports uridine (Wang et al., 1997). hCNT3 is broadly selective, transporting both purine and pyrimidine nucleosides with high affinities (Ritzel et al., 2001). The Na⁺-nucleoside coupling ratio for hCNT1 and hCNT2 is 1:1 whereas hCNT3 has a Na⁺-nucleoside ratio of 2:1 and H⁺-nucleoside ratio of 1:1 (Smith et al., 2005).

Although the permeant selectivities of hNTs have been extensively characterized for many nucleoside analogs, relatively little is known about how hNTs transport FLT. The main objectives of the current study were to determine how well the hNTs interact with and transport FLT and to determine which hNTs are important for FLT uptake in various human cancer cell lines. Using ³H-FLT to follow cellular uptake, we show that FLT was transported by hENT1, hENT2, hCNT1 and hCNT3 and that hENT1 was responsible for the majority of hNT-mediated ³H-FLT uptake in the cell lines tested. In five of the six cell lines tested, a strong correlation was observed between the abundance of hENT1 at the extracellular surface and FLT uptake.

MOL #48900

Materials and Methods

Materials

[Methyl-³H(N)]-3'-deoxy-3'-fluorothymidine (³H-FLT; 126 GBq/mmol), [methyl-³H]-thymidine (³H-thymidine; 2.25 TBq/mmol), [5, 6-³H]-uridine (³H-uridine; 1.31 TBq/mmol), and [³H(G)]-S-(p-nitrobenzyl)-6-thioinosine (³H-NBMPR; 555 GBq/mmol) were purchased from Moravek Biochemicals (Brea, CA). Research grade thymidine, uridine, FLT, N-methyl-D-glucamine (NMDG), dilazep, and NBMPR were purchased from Sigma-Aldrich (St. Louis, MO). All other reagents were of analytical grade and were purchased from commercial sources.

Inhibitor-Sensitivity Assays with hNT-Producing Yeast Cells

Inhibitor-sensitivity assays were performed as previously described (Vickers et al., 2004; Zhang et al., 2003). Briefly, yeast cultures producing recombinant hNTs (see (Visser et al., 2002; Zhang et al., 2005; Zhang et al., 2003) for construction of yeast strains) were maintained in complete minimal medium (CMM) containing 0.67% (w/v) yeast nitrogen base (Difco, Detroit, MI), amino acids (to maintain auxotrophic selection) and 2% (w/v) glucose (CMM/GLU). Yeast cells were washed three times with CMM/GLU (pH 7.4), resuspended to an OD₆₀₀ of 4, and added to “preloaded” 96-well plates containing CMM/GLU (pH 7.4) with either FLT or thymidine (at desired concentrations) and ³H-uridine. Non-specific binding and uptake of ³H-uridine were determined by incubating wells with 10 mM uridine. Mediated ³H-uridine transport was determined by the difference of ³H-uridine uptake between cells in the absence and presence of 10 mM uridine. Yeast cells producing recombinant hENT1, hENT2, hCNT1, hCNT2, or hCNT3 were incubated with ³H-uridine for 20, 20, 30, 30, or 10 min, respectively. Yeast cells producing hCNT3 displayed greater ³H-uridine transport than the other yeast strains and were therefore incubated with ³H-uridine for a shorter duration than the other yeast strains. After incubation, yeast cells were harvested and washed with a Micro96 Harvester (Skatron Intruments, Lier, Norway) and radioactivity in yeast cells was determined by liquid scintillation counting (LS 6500, Beckman Coulter, Fullerton, CA). IC₅₀ values (concentration of thymidine or FLT that inhibited 50% of ³H-uridine uptake) were determined and converted to K_i values using the Cheng-Prusoff equation (Cheng and Prusoff, 1973),

MOL #48900

$K_i = IC_{50}/(1+([L]/K_m))$ in which [L] was the concentration of ^3H -uridine (1 μM) and apparent K_m values were determined in previous publications [hENT1, 43 μM ; hENT2, 190 μM ; hCNT1, 9.2 μM ; hCNT2, 29 μM ; hCNT3, 8.7 μM (Vickers et al., 2004; Zhang et al., 2005; Zhang et al., 2003)]. Unless otherwise indicated, all data were analyzed using GraphPad Prism version 4 software (GraphPad Software Inc, San Diego, CA).

Transport Assays in hNT-producing *Xenopus laevis* oocytes

hNT cDNAs in the *Xenopus* expression vector pGEM-HE were transcribed with T7 polymerase using the mMMESSAGE mMACHINETM (Ambion) transcription system, and produced in oocytes of *Xenopus laevis* by standard procedures (Yao et al., 2000). Healthy defolliculated stage VI oocytes were microinjected with 20 nl water or 20 nl water containing RNA transcripts (20 ng) and incubated in modified Barth's medium (changed daily) at 18°C for 72 h prior to the assay of transport activity

Transport assays were performed at room temperature (20°C) on groups of 10-12 oocytes in 200 μl transport buffer as previously described (King et al., 2006). Incubations were for 30 min to measure cellular uptake, and 1 min to measure initial rates of transport. Except where otherwise indicated, the concentration of radiolabeled permeant was 20 μM . Following incubation periods, oocytes were rapidly washed six times in ice-cold transport medium to remove extracellular radioactivity. Oocytes were dissolved in 5% (w/v) sodium dodecyl sulfate and measured for radioactivity by liquid scintillation counting. Presented as pmol/oocyte/30 min (cellular uptake) or pmol/oocyte/min (initial rate of transport), values were corrected for non-mediated uptake measured in control, water-injected oocytes.

Cell Culture

Due to the potential utility of FLT-PET in lung, breast, and brain cancers (Been et al., 2004), A549, MCF-7, and U251 cells (derived from a lung carcinoma, breast adenocarcinoma, and glioblastoma, respectively) were used in this study. In addition, the pancreatic carcinoma cell lines MIA PaCa-2 and Capan-2 were tested since FLT-PET may have applications in treatment planning of pancreatic cancer and the renal carcinoma cell line A498 was tested because it is one of the few cell lines known to possess hCNT3, which is capable of transporting FLT, and FLT-PET may be useful for detecting renal tumors

MOL #48900

(Lawrentschuk et al., 2006). MCF-7, A549, U251, and A498 cells were maintained in RPMI 1640 medium containing 10% (v/v) fetal bovine serum (FBS). MIA PaCa-2 cells were maintained in Dulbecco's modified Eagle's medium with 4.5 g/l glucose, 1.5 g/l sodium bicarbonate, 10% (v/v) FBS, and 2.5% (v/v) horse serum. Capan-2 cells were maintained in McCoy's 5A medium with 10% (v/v) FBS. For all transport and binding experiments, cells were inoculated in 12-well plates at 5×10^4 (MCF-7 and Capan-2), 4×10^4 (U251 and A498), 3×10^4 (MIA PaCa-2), and 2.5×10^4 (A549) cells/well. Cultures reached ~50% confluency after plates were incubated at 37°C with 5% CO₂ for 72 h at which point cells were used for equilibrium binding or uptake assays.

Quantitative Real-Time RT-PCR

RNA was isolated from cell lines using the RNeasy kit (Qiagen, Mississauga, Ontario) and 2 µg RNA for each reaction was reverse transcribed into DNA using the TaqMan Gold RT-PCR kit (Applied Biosystems, Foster City, CA) following the manufacturer's instructions. For each real-time PCR reaction, cDNA (0.53 µl/well) was added to 2x TaqMan Universal PCR Master Mix (Applied Biosystems, Foster City, CA), that contained primers and probes (see Table 1) in a final volume of 20 µl/well. Reactions were run in triplicate on 96-well plates using an Applied Biosystems 7900HT Fast Real-Time PCR system (Applied Biosystems, Foster City, CA) using standard default settings. Relative quantification of RNA was determined using the delta-delta C_T method (Livak and Schmittgen, 2001) using glyceraldehyde-3-phosphate dehydrogenase (GAPDH) to control for RNA loading differences. Validation assays demonstrated that the genes analyzed in this study were amplified with equal efficiencies (data not shown).

Radiotracer Uptake Assays with Cell Lines

Cells in 12-well plates were washed once (1 ml/well) with either Na⁺ buffer (20 mM Tris, 3 mM K₂HPO₄, 5 mM glucose, and 145 mM NaCl) or NMDG buffer (20 mM Tris, 3 mM K₂HPO₄, 5 mM glucose, and 155 mM NMDG). Cells were incubated for up to 45 min with 0.5 ml/well Na⁺ or NMDG buffer with or without hNT inhibitors (NBMPR or dilazep) to allow interaction between inhibitors and hNTs. Cells were then incubated with 0.5 ml/well Na⁺ or NMDG buffer containing 147 nM ³H-thymidine

MOL #48900

or ^3H -FLT (9.25 kBq/well [0.25 μCi /well]) for 60 min at 37°C. After incubation, radioactive buffer was removed and cells were washed once with either Na^+ or NMDG buffer. Cells were solubilized by the addition of 0.5 ml/well 0.5 M KOH for 45 min and the resulting KOH solutions were analyzed for radioactivity by liquid scintillation counting. Protein content in the KOH solutions was determined by the Bio-Rad Protein Assay (Bio-Rad, Hercules, CA).

The role of hENT1 in the uptake of FLT was determined by assessing ^3H -FLT uptake in graded NBMPR concentrations (0.003 – 100 nM). Cells in 12-well plates were washed once with Na^+ buffer and incubated for 60 min at 37°C with 1 ml/well Na^+ buffer containing graded NBMPR concentrations and 74 nM ^3H -FLT with or without 200 μM dilazep and 10 mM uridine. Mediated ^3H -FLT uptake was determined from the difference in ^3H -FLT uptake between cells incubated without (total) or with 200 μM dilazep and 10 mM uridine (non-mediated). ^3H -FLT uptake inhibited by NBMPR was analyzed in concentration-effect curves, where 100% and 0% uptake represented the largest and smallest amounts of ^3H -FLT uptake observed, respectively, over the graded concentrations of NBMPR.

Equilibrium Binding Assays with Cell Lines

Cells in 12-well plates were washed with Na^+ buffer and then incubated for 90 min at 37°C with 1 ml/well Na^+ buffer containing graded concentrations (0.1 – 2.5 nM) of ^3H -NBMPR in the presence or absence of 1 μM NBMPR. After incubation, 50- μl aliquots were removed from each well to determine the free concentration of ^3H -NBMPR. Radioactive buffer was removed and cells were washed and then incubated with 0.5 ml/well 0.5 M KOH for 45 min and radioactive content was determined by liquid scintillation counting. Binding of ^3H -NBMPR to cells in the presence or absence of 1 μM NBMPR represented non-specific and total binding, respectively, and the difference between the two, which represented site-specific binding, was used to determine binding parameters (B_{max} and K_d values).

Equilibrium binding experiments were also performed using FTH-SAENTA to determine the relative proportions of extracellular and intracellular NBMPR binding sites. FTH-SAENTA, being membrane impermeable, has been shown to interact only with the extracellular NBMPR binding sites (Visser et al., 2007). Cells in 12-well plates were washed twice and then incubated for 60 min with 1

MOL #48900

ml/well Na⁺ buffer containing 10 nM ³H-NBMMPR alone, 10 nM ³H-NBMMPR with 100 nM FTH-SAENTA, or 10 nM ³H-NBMMPR with 10 μM NBMMPR. Cells were washed three times followed by solubilization with 1 ml/well 5% Triton X-100 for at least 2 h. The radioactive content of the solubilized material was determined by liquid scintillation counting. Total specifically bound ³H-NBMMPR (extracellular and intracellular) was calculated from the difference between ³H-NBMMPR bound in the presence and absence 10 μM NBMMPR. Extracellular specifically bound ³H-NBMMPR was calculated from the difference of ³H-NBMMPR bound with or without FTH-SAENTA. The percentage of specifically bound extracellular ³H-NBMMPR was calculated as (extracellular/total bound ³H-NBMMPR) x 100.

MOL #48900

Results

Interaction of FLT with Recombinant hNTs in Yeast Cells

Zhang et al. developed an assay that assesses the ability of nucleoside analogs to inhibit uridine uptake by yeast producing various recombinant hNTs that provides a measure of the apparent affinities of the hNTs for nucleoside analogs (Zhang et al., 2005; Zhang et al., 2003). Graded concentrations of thymidine and FLT were used to inhibit ^3H -uridine uptake in yeast cells producing individual hNTs (Fig. 1) to determine IC_{50} values (concentration of thymidine or FLT that inhibited ^3H -uridine uptake by 50%) that were converted to K_i values. Thymidine K_i values for hENT1, hENT2, hCNT1, hCNT2, and hCNT3 were 74 ± 17 , 160 ± 10 , 20 ± 3 , 1200 ± 200 , and 31 ± 5 , respectively. FLT displayed K_i values for hENT1, hENT2, hCNT1, hCNT2, and hCNT3 that were 12-, 3.4-, 5.0-, >8.3-, and 15-fold larger than thymidine K_i values, respectively, suggesting that substitution of fluorine for the 3'-hydroxyl group significantly decreased the affinities of the hNTs for FLT. hCNT1 displayed the lowest K_i value (i.e., highest apparent affinity) for FLT, followed by hCNT3, hENT2, hENT1 and hCNT2.

Transportability of FLT by Recombinant hNTs in Oocytes

Xenopus laevis oocytes, which have low endogenous transport of nucleosides (Jarvis and Griffith, 1991), have been extensively used to assess membrane transport of nucleosides and nucleoside analogs by recombinant hNTs. Values for mediated ^3H -FLT uptake in *Xenopus* oocytes producing recombinant hNTs were robust and relatively similar to those of ^3H -thymidine (Fig. 2A). When hNT-producing oocytes were incubated with $20 \mu\text{M}$ ^3H -FLT, hCNT1 displayed the greatest (pmol/oocyte/30 min) FLT uptake (48 ± 8), followed by hCNT3 (32 ± 5), hENT2 (12 ± 1), hENT1 (11 ± 0.8), and hCNT2 (2.0 ± 0.2). The weak interaction between FLT and hCNT2 likely explains the poor transportability of ^3H -FLT by hCNT2. Compared to ^3H -thymidine, ^3H -FLT displayed 3.4-fold greater uptake in water injected oocytes (data not shown), suggesting ^3H -FLT underwent a greater amount of passive diffusion across oocyte membranes.

Influx of ^3H -FLT by hENT1, hENT2, hCNT1 and hCNT3 was concentration dependent and conformed to Michaelis-Menten kinetics (Fig. 2B); the K_m and V_{max} values are presented in Table 2. hENT1 and hENT2 displayed greater transport capacities and lower apparent affinities (larger V_{max} and K_m

MOL #48900

values, respectively) for ^3H -FLT than hCNT1 and hCNT3. The V_{\max}/K_m ratio, a measure of transport efficiency, was about 6-fold greater for hCNT1 and hCNT3 than for hENT1 and hENT2, suggesting that hCNT1 and hCNT3 transport ^3H -FLT more efficiently than hENT1 and hENT2 at lower (μM) concentrations.

Relative Quantification of hNTs in Cell Lines

Since FLT was shown to be a permeant of several recombinant hNTs, it was expected that cellular accumulation of FLT would be influenced by expression of hNT transcripts in the cancer cell lines used in this study. Relative quantification of hNT-transcript levels was determined by real-time PCR (Fig. 3). All genes analyzed were amplified with equal efficiencies and GAPDH was used as the RNA loading control. Transcript levels of hENT1 were 7-, 11-, 25-, and 340-fold greater than those of hENT2, the second most abundant hNT, in A549, MIA PaCa-2, U251, and A498 cells, respectively, whereas transcript levels of hENT2 were equal to and 3-fold greater than those of hENT1 in MCF-7 and Capan-2 cells, respectively. For all cell lines, hENT1 transcripts were at least 300-fold greater than hCNT1/2/3 transcripts and only hCNT2 was detectable in A549 cells, suggesting that hCNT1, hCNT2 and hCNT3 play minor roles in cellular uptake of nucleosides in the cell lines tested.

hNTs Responsible for ^3H -FLT Uptake in Cell Lines

^3H -FLT uptake assays were performed in different transport buffers to determine the functional hNTs that were involved in ^3H -FLT uptake (Figure 4A). Na^+ buffer allowed tracer uptake mediated by both hENTs and hCNTs while NMDG buffer, which lacks Na^+ , allowed tracer uptake mediated by only hENTs. Buffers with 100 μM dilazep inhibited both hENT1 and hENT2 transport while buffers with 100 nM NBMPR inhibited only hENT1 transport. NMDG buffer with 200 μM dilazep and 10 mM uridine was used to determine non-mediated tracer uptake. ^3H -FLT uptake in NMDG buffer was 76, 78, 90, and 98% of uptake in Na^+ -containing buffer for Capan-2, A549, MCF-7, and U251 cells, respectively, suggesting that hCNTs were relatively unimportant for ^3H -FLT uptake in these cell lines. Addition of 100 nM NBMPR to Na^+ buffer reduced mediated ^3H -FLT uptake (determined by the difference of ^3H -FLT uptake in buffers with or without 200 μM dilazep and 10 mM uridine) by 50, 63, 68, 71, 77, and 77% in Capan-2,

MOL #48900

MCF-7, U251, A549, MIA PaCa-2, and A-498 cells, respectively, suggesting that hENT1 was the main hNT involved in ^3H -FLT uptake in these cell lines (Fig. 4B).

NBMPR Binding and Inhibition of ^3H -FLT Uptake in Cell Lines

To determine the importance of hENT1 for ^3H -FLT uptake in the cell lines used in this study, ^3H -NBMPR equilibrium binding assays (Fig. 5A) and concentration-effect assays with NBMPR inhibiting ^3H -FLT uptake (Fig. 5B) were performed. ^3H -NBMPR binding parameters are displayed in Table 3. NBMPR B_{max} values varied significantly between cell lines (180 – 1300 fmol/ 10^6 cells). MIA PaCa-2 cells displayed the largest amount of NBMPR binding sites, followed by MCF-7, A549, U251, A498, and Capan-2. Unlike B_{max} values, the K_d values were similar for all of the cell lines (0.18 – 0.43 nM). When comparing NBMPR, K_d and IC_{50} values (Table 3), MCF-7, A549, and Capan-2 cells displayed IC_{50} values smaller or equal to K_d values, suggesting that binding and inhibition of 50% of hENT1 transporters by NBMPR decreased NBMPR-sensitive FLT uptake by at least 50%.

Cellular hENT1 Location in Cell Lines

Although hENT1 is considered a plasma membrane transporter, it has been found in nuclear and mitochondrial membranes (Lai et al., 2004; Mani et al., 1998). To determine the proportions of intracellular and extracellular NBMPR binding sites (i.e., hENT1 on intracellular and plasma membranes, respectively), ^3H -NBMPR equilibrium binding assays were performed with or without FTH-SAENTA (Fig. 6). Unlike NBMPR, FTH-SAENTA is membrane impermeable and can only bind hENT1 on the extracellular surface of the plasma membrane, thereby allowing quantification of extracellular and intracellular NBMPR binding sites (Table 3). MCF-7 cells had the greatest percentage of NBMPR binding sites on extracellular surfaces, followed by A549, MIA PaCa-2, U251, A498, and Capan-2 cells. MIA PaCa-2 displayed the greatest number of extracellular NBMPR binding sites ($4.4 \times 10^5 \pm 7 \times 10^4$ sites/cell), which was 2.3-, 3.4-, 4.5-, 7.2-, and 220-fold greater than the extracellular NBMPR binding sites for MCF-7, A549, U251, A498, and Capan-2 cells, respectively.

Relationship Between FLT Uptake and Extracellular NBMPR Binding Sites

MOL #48900

There was a strong correlation between FLT uptake and extracellular NBMPR binding sites/cell in five of the six cell lines used in this study ($P = 0.0011$, $r^2 = 0.98$, Fig. 7). MIA PaCa-2, which was excluded from Fig. 7, had at least a 2-fold greater number of extracellular NBMPR binding sites than any other cell line in this study but had similar FLT uptake to U251. For all cells lines except MIA PaCa-2, there was a clear relationship between the levels of extracellular plasma membrane hENT1 and FLT uptake.

MOL #48900

Discussion

FLT-PET has been demonstrated useful for determining the proliferative status of various tumor types (Been et al., 2004). Although FLT metabolism is generally considered the rate-limiting step for cellular FLT accumulation, some studies have suggested the importance of FLT transport for FLT accumulation. RIF-1 xenograft tumors in mice displayed a 1.8-fold increase in ^{18}F -FLT uptake when tumor-bearing mice were given an i.p. dose of 5-fluorouracil (Perumal et al., 2006). Although RIF-1 tumors displayed no change in TK1 protein or ATP levels, NBMPR binding to cultured RIF-1 cells increased 50% after a 2-h incubation with 10 $\mu\text{g/ml}$ 5-fluorouracil, suggesting that FLT transport was the rate-limiting process for FLT accumulation in RIF-1 tumors. However, the increased tumor uptake of ^{18}F -FLT may have been caused by depletion of cellular TMP pools due to inhibition of thymidylate synthase, which produces TMP from dUMP. Decreased TMP pools allow greater phosphorylation of FLT-monophosphate to FLT-diphosphate by thymidylate kinase, which is the rate-limiting enzyme involved in FLT metabolism (Grierson et al., 2004).

The current study examined interactions between hNTs and FLT and determined which hNTs were capable of mediating FLT transport. Substitution of the 3'-hydroxyl group of thymidine with a fluoro group increased K_i values for inhibition of uridine transport (a measure of interaction with hNTs) by 3- to 15-fold. This reduction in hNTs' apparent affinities for FLT was relatively small considering the importance of the 3'-hydroxyl group in uridine for nucleoside-hNT interaction - i.e., using the yeast inhibitor-sensitivity assay described herein, hCNT3, hENT1, hCNT2, and hCNT1 displayed, respectively, 39-, >54-, >107-, and 135-fold larger K_i values for 3'-deoxyuridine than for uridine (Vickers et al., 2004; Zhang et al., 2003). FLT interacted poorly with hCNT2, and this explains the low amount of FLT uptake observed in oocytes producing hCNT2. It was surprising to observe that rates of ^3H -FLT uptake were equal or greater than rates of ^3H -thymidine uptake in oocytes producing hCNT1, hENT1, hENT2, and hENT3 since in most cultured cell lines ^3H -thymidine accumulates to a greater extent than ^3H -FLT (Toyohara et al., 2002). However, differences in nucleoside metabolism in mammalian cells and *Xenopus laevis* oocytes may explain the differences in rates of ^3H -FLT and ^3H -thymidine uptake in oocytes, since

MOL #48900

Xenopus laevis oocytes display little thymidine metabolism (Jarvis and Griffith, 1991). To the authors' knowledge, there is no information regarding oocyte metabolism of FLT.

Analysis of hNT transcript levels by real-time PCR revealed relatively little hCNT mRNA expression in the six cell lines. These results are supported by the small changes in ^3H -FLT uptake displayed when most of the cell lines were incubated in NMDG buffer. A notable exception was MIA PaCa-2 cells, which displayed 59% ^3H -FLT uptake in NMDG buffer compared to Na^+ buffer, suggesting that 41% of ^3H -FLT uptake was mediated by hCNTs. However, MIA PaCa-2 cells incubated in Na^+ buffer with 100 μM dilazep displayed 17% ^3H -FLT uptake compared to Na^+ buffer alone, suggesting that 83% of ^3H -FLT uptake was mediated by hENTs. The basis of this discrepancy in hNT activity in MIA PaCa-2 cells remains unclear and warrants further investigation. Although MIA PaCa-2 and Capan-2 were both pancreatic carcinoma cell lines, their hNT transcript expression patterns differed significantly. MIA PaCa-2 and Capan-2 displayed hENT1/hENT2 expression ratios of 11 and 0.35, respectively, demonstrating that hNT expression patterns may differ between cell lines of similar origin.

For all cell lines, incubation of NBMPR in Na^+ buffer reduced hNT-mediated ^3H -FLT uptake by at least 50%, suggesting that hENT1 was the predominant hNT involved in ^3H -FLT uptake. Although hCNTs appeared to have greater affinities for FLT, the greater abundance of hENT1 in the cell lines studied resulted in its mediating the greatest amount of ^3H -FLT uptake. For MCF-7, A549, and Capan-2 cells, inhibition of 50% hENT1 decreased hENT1-mediated ^3H -FLT uptake by at least 50%, suggesting that changes in transport activities in these cell lines had an immediate effect on FLT uptake. For the other cell lines, FLT phosphorylation may be the rate-limiting process for FLT uptake and upon inhibition of a subset of hENT1 by NBMPR, FLT transport may become the rate-limiting process for FLT uptake.

For all cell lines except MIA PaCa-2, a strong correlation was observed between extracellular NBMPR binding sites and ^3H -FLT uptake. MIA PaCa-2 displayed more than two-fold larger number of extracellular NBMPR binding sites than the other cell lines but did not display proportionally greater FLT uptake, suggesting that FLT phosphorylation was the rate-limiting step for FLT uptake in MIA PaCa-2. When analyzing TK1 mRNA levels using real-time PCR for MIA PaCa-2, Capan-2, and MCF-7, TK1

MOL #48900

mRNA levels in MIA PaCa-2 were 26% and 17% of those found in Capan-2 and MCF-7, respectively (data not shown), suggesting MIA PaCa-2 had low levels of TK1.

Understanding membrane transport of FLT in cells may explain the relatively low sensitivity of FLT-PET compared to the commonly used fluorodeoxyglucose (FDG)-PET. Immunohistochemical staining of hENT1 in 33 frozen sections of primary breast cancers revealed significant variations in hENT1 staining between tumors. Using a 0-4+ intensity staining scale, 4, 5, 7, 14, and 3 sections scored 0, 1+, 2+, 3+, and 4+, respectively (Mackey et al., 2002). No detectable hENT1 staining was observed in 12% of tumors examined, suggesting that FLT-PET may provide false-negative images for these tumors. Data from FLT-PET pilot studies in breast cancer patients suggested that 7-20% of tumors are not detectable by FLT-PET (Been et al., 2006; Smyczek-Gargya et al., 2004). These tumors may have low levels of hENT1, explaining their unobservable nature in FLT-PET.

hNT levels are variable in almost all cancers studied. RNA analysis of four pancreatic cell lines (NP9, NP18, NP29, and NP31) revealed that hENT1, hENT2, hCNT1, hCNT2, and hCNT3 mRNA levels differed significantly between the four cell lines and only hENT1 mRNA was easily detectable for all four cell lines (Garcia-Manteiga et al., 2003). When hENT1 levels were analyzed in 21 pancreatic adenocarcinomas using immunohistochemistry, 12 samples displayed no detectable hENT1 in 10-100% of adenocarcinoma cells, suggesting that hENT1 is not present in all pancreatic adenocarcinomas (Spratlin et al., 2004). Variability in ¹⁸F-FLT uptake between tumors may be partly explained by the considerable inter-individual variability in tumor hNT levels (Pennycooke et al., 2001). When comparing RNA levels for hENT1 using matched tumor/normal tissue individual arrays, there was no consistent difference in hENT1 expression levels for kidney, breast, uterus, ovary, colon, lung, stomach, and rectum (Pennycooke et al., 2001). Only prostate tumors consistently demonstrated decreased hENT1 expression compared to normal tissues (hENT1 tumor levels 47% of normal tissues). These same prostate arrays also exhibited consistently higher levels of hENT2 tumor expression (hENT2 tumor levels 323% of normal tissues), suggesting prostate tumors still retain the capacity for FLT transport despite the decrease in hENT1 levels. hCNT1 was not detectable in the majority of the matched tissue arrays (breast, prostate, cervix, colon,

MOL #48900

stomach, and rectum) and consistently displayed low levels of tumor expression in almost all other tested tissues (kidney, uterus, lung, and small intestine), suggesting that neoplastic transformation of these tissues may decrease capacity for FLT transport.

It is interesting to note that cellular hENT1 levels correlated with FLT uptake (present study) and the therapeutic activity of gemcitabine in pancreatic adenocarcinomas (Spratlin et al., 2004). Patients with pancreatic adenocarcinoma tumors in which over 90% of tumor cells displayed hENT1 staining had significantly longer median survival times after gemcitabine monotherapy than patients with tumors in which 0-90% of tumor cells displayed hENT1 staining. If hENT1 levels influence both FLT uptake and gemcitabine cytotoxicity in pancreatic cancers, perhaps FLT-PET would be useful to determine gemcitabine resistance in pancreatic cancers prior to gemcitabine treatment. Further studies are required to validate this hypothesis.

Prior to this study, only hENT1 was known to transport FLT across plasma membranes and it was unknown whether the other hNTs could transport FLT (Kong et al., 1992). The current study has determined that FLT can interact with and is transported by hENT1, hENT2, hCNT1 and hCNT3. Because of the greater relative abundance of hENT1 in the tested cell lines, ³H-FLT uptake was primarily mediated by hENT1. Small alterations of hENT1 transport activity by treatment with NBMPR reduced ³H-FLT uptake in MCF-7, A549, and Capan-2 cells. A strong correlation was observed between ³H-FLT uptake and the number of extracellular NBMPR binding sites/cell for five of the six cell lines tested, demonstrating the importance of hENT1 for FLT uptake.

MOL #48900

Acknowledgments

We thank Delores Mowles and Jolanta Alcaraz-Limcangco for their dedicated support in laboratory maintenance.

MOL #48900

References

- Baldwin SA, Yao SY, Hyde RJ, Ng AM, Foppolo S, Barnes K, Ritzel MW, Cass CE and Young JD (2005) Functional characterization of novel human and mouse equilibrative nucleoside transporters (hENT3 and mENT3) located in intracellular membranes. *J Biol Chem* **280**(16):15880-15887.
- Barnes K, Dobrzynski H, Foppolo S, Beal PR, Ismat F, Scullion ER, Sun L, Tellez J, Ritzel MW, Claycomb WC, Cass CE, Young JD, Billeter-Clark R, Boyett MR and Baldwin SA (2006) Distribution and functional characterization of equilibrative nucleoside transporter-4, a novel cardiac adenosine transporter activated at acidic pH. *Circ Res* **99**(5):510-519.
- Barthel H, Perumal M, Latigo J, He Q, Brady F, Luthra SK, Price PM and Aboagye EO (2005) The uptake of 3'-deoxy-3'-[18F]fluorothymidine into L5178Y tumours in vivo is dependent on thymidine kinase 1 protein levels. *Eur J Nucl Med Mol Imaging* **32**(3):257-263.
- Been LB, Elsinga PH, de Vries J, Cobben DC, Jager PL, Hoekstra HJ and Suurmeijer AJ (2006) Positron emission tomography in patients with breast cancer using (18)F-3'-deoxy-3'-fluoro-l-thymidine ((18)F-FLT)-a pilot study. *Eur J Surg Oncol* **32**(1):39-43.
- Been LB, Suurmeijer AJ, Cobben DC, Jager PL, Hoekstra HJ and Elsinga PH (2004) [18F]FLT-PET in oncology: current status and opportunities. *Eur J Nucl Med Mol Imaging* **31**(12):1659-1672.
- Cheng Y and Prusoff WH (1973) Relationship between the inhibition constant (K₁) and the concentration of inhibitor which causes 50 per cent inhibition (I₅₀) of an enzymatic reaction. *Biochem Pharmacol* **22**(23):3099-3108.
- Garcia-Manteiga J, Molina-Arcas M, Casado FJ, Mazo A and Pastor-Anglada M (2003) Nucleoside transporter profiles in human pancreatic cancer cells: role of hCNT1 in 2',2'-difluorodeoxycytidine- induced cytotoxicity. *Clin Cancer Res* **9**(13):5000-5008.
- Grierson JR, Schwartz JL, Muzi M, Jordan R and Krohn KA (2004) Metabolism of 3'-deoxy-3'-[F-18]fluorothymidine in proliferating A549 cells: validations for positron emission tomography. *Nucl Med Biol* **31**(7):829-837.
- Griffiths M, Beaumont N, Yao SY, Sundaram M, Boumah CE, Davies A, Kwong FY, Coe I, Cass CE, Young JD and Baldwin SA (1997a) Cloning of a human nucleoside transporter implicated in the cellular uptake of adenosine and chemotherapeutic drugs. *Nat Med* **3**(1):89-93.
- Griffiths M, Yao SY, Abidi F, Phillips SE, Cass CE, Young JD and Baldwin SA (1997b) Molecular cloning and characterization of a nitrobenzylthioinosine-insensitive (ei) equilibrative nucleoside transporter from human placenta. *Biochem J* **328** (Pt 3):739-743.
- Jarvis SM and Griffith DA (1991) Expression of the rabbit intestinal N² Na⁺/nucleoside transporter in *Xenopus laevis* oocytes. *Biochem J* **278** (Pt 2):605-607.
- King KM, Damaraju VL, Vickers MF, Yao SY, Lang T, Tackaberry TE, Mowles DA, Ng AM, Young JD and Cass CE (2006) A comparison of the transportability, and its role in cytotoxicity, of clofarabine, cladribine, and fludarabine by recombinant human nucleoside transporters produced in three model expression systems. *Mol Pharmacol* **69**(1):346-353.
- Kong W, Engel K and Wang J (2004) Mammalian nucleoside transporters. *Curr Drug Metab* **5**(1):63-84.
- Kong XB, Zhu QY, Vidal PM, Watanabe KA, Polsky B, Armstrong D, Ostrander M, Lang SA, Jr., Muchmore E and Chou TC (1992) Comparisons of anti-human immunodeficiency

MOL #48900

- virus activities, cellular transport, and plasma and intracellular pharmacokinetics of 3'-fluoro-3'-deoxythymidine and 3'-azido-3'-deoxythymidine. *Antimicrob Agents Chemother* **36**(4):808-818.
- Lai Y, Tse CM and Unadkat JD (2004) Mitochondrial expression of the human equilibrative nucleoside transporter 1 (hENT1) results in enhanced mitochondrial toxicity of antiviral drugs. *J Biol Chem* **279**(6):4490-4497.
- Latini S and Pedata F (2001) Adenosine in the central nervous system: release mechanisms and extracellular concentrations. *J Neurochem* **79**(3):463-484.
- Lawrentschuk N, Poon AM and Scott AM (2006) Fluorine-18 Fluorothymidine: A New Positron Emission Radioisotope for Renal Tumors. *Clin Nucl Med* **31**(12):788-789.
- Livak KJ and Schmittgen TD (2001) Analysis of relative gene expression data using real-time quantitative PCR and the 2(-Delta Delta C(T)) Method. *Methods* **25**(4):402-408.
- Mackey JR, Baldwin SA, Young JD and Cass CE (1998) Nucleoside transport and its significance for anticancer drug resistance. *Drug Resistance Updates* **1**:310-324.
- Mackey JR, Jennings LL, Clarke ML, Santos CL, Dabbagh L, Vsianska M, Koski SL, Coupland RW, Baldwin SA, Young JD and Cass CE (2002) Immunohistochemical variation of human equilibrative nucleoside transporter 1 protein in primary breast cancers. *Clin Cancer Res* **8**(1):110-116.
- Mani RS, Hammond JR, Marjan JM, Graham KA, Young JD, Baldwin SA and Cass CE (1998) Demonstration of equilibrative nucleoside transporters (hENT1 and hENT2) in nuclear envelopes of cultured human choriocarcinoma (BeWo) cells by functional reconstitution in proteoliposomes. *J Biol Chem* **273**(46):30818-30825.
- Pastor-Anglada M, Felipe A and Casado FJ (1998) Transport and mode of action of nucleoside derivatives used in chemical and antiviral therapies. *Trends Pharmacol Sci* **19**(10):424-430.
- Pennycooke M, Chaudary N, Shuralyova I, Zhang Y and Coe IR (2001) Differential expression of human nucleoside transporters in normal and tumor tissue. *Biochem Biophys Res Commun* **280**(3):951-959.
- Perumal M, Pillai RG, Barthel H, Leyton J, Latigo JR, Forster M, Mitchell F, Jackman AL and Aboagye EO (2006) Redistribution of nucleoside transporters to the cell membrane provides a novel approach for imaging thymidylate synthase inhibition by positron emission tomography. *Cancer Res* **66**(17):8558-8564.
- Rasey JS, Grierson JR, Wiens LW, Kolb PD and Schwartz JL (2002) Validation of FLT uptake as a measure of thymidine kinase-1 activity in A549 carcinoma cells. *J Nucl Med* **43**(9):1210-1217.
- Ritzel MW, Ng AM, Yao SY, Graham K, Loewen SK, Smith KM, Ritzel RG, Mowles DA, Carpenter P, Chen XZ, Karpinski E, Hyde RJ, Baldwin SA, Cass CE and Young JD (2001) Molecular identification and characterization of novel human and mouse concentrative Na⁺-nucleoside cotransporter proteins (hCNT3 and mCNT3) broadly selective for purine and pyrimidine nucleosides (system cib). *J Biol Chem* **276**(4):2914-2927.
- Ritzel MW, Yao SY, Huang MY, Elliott JF, Cass CE and Young JD (1997) Molecular cloning and functional expression of cDNAs encoding a human Na⁺-nucleoside cotransporter (hCNT1). *Am J Physiol Cell Physiol* **272**(2):707-714.
- Shryock JC and Belardinelli L (1997) Adenosine and adenosine receptors in the cardiovascular system: biochemistry, physiology, and pharmacology. *Am J Cardiol* **79**(12A):2-10.

MOL #48900

- Smith KM, Slugoski MD, Loewen SK, Ng AM, Yao SY, Chen XZ, Karpinski E, Cass CE, Baldwin SA and Young JD (2005) The broadly selective human Na⁺/nucleoside cotransporter (hCNT3) exhibits novel cation-coupled nucleoside transport characteristics. *J Biol Chem* **280**(27):25436-25449.
- Smyczek-Gargya B, Fersis N, Dittmann H, Vogel U, Reischl G, Machulla HJ, Wallwiener D, Bares R and Dohmen BM (2004) PET with [¹⁸F]fluorothymidine for imaging of primary breast cancer: a pilot study. *Eur J Nucl Med Mol Imaging* **31**(5):720-724.
- Spratlin J, Sangha R, Glubrecht D, Dabbagh L, Young JD, Dumontet C, Cass C, Lai R and Mackey JR (2004) The absence of human equilibrative nucleoside transporter 1 is associated with reduced survival in patients with gemcitabine-treated pancreas adenocarcinoma. *Clin Cancer Res* **10**(20):6956-6961.
- Toyohara J, Waki A, Takamatsu S, Yonekura Y, Magata Y and Fujibayashi Y (2002) Basis of FLT as a cell proliferation marker: comparative uptake studies with [³H]thymidine and [³H]arabinothymidine, and cell-analysis in 22 asynchronously growing tumor cell lines. *Nucl Med Biol* **29**(3):281-287.
- Vickers MF, Zhang J, Visser F, Tackaberry T, Robins MJ, Nielsen LP, Nowak I, Baldwin SA, Young JD and Cass CE (2004) Uridine recognition motifs of human equilibrative nucleoside transporters 1 and 2 produced in *Saccharomyces cerevisiae*. *Nucleosides Nucleotides Nucleic Acids* **23**(1-2):361-373.
- Visser F, Sun L, Damaraju V, Tackaberry T, Peng Y, Robins MJ, Baldwin SA, Young JD and Cass CE (2007) Residues 334 and 338 in transmembrane segment 8 of human equilibrative nucleoside transporter 1 are important determinants of inhibitor sensitivity, protein folding, and catalytic turnover. *J Biol Chem* **282**(19):14148-14157.
- Visser F, Vickers MF, Ng AM, Baldwin SA, Young JD and Cass CE (2002) Mutation of residue 33 of human equilibrative nucleoside transporters 1 and 2 alters sensitivity to inhibition of transport by dilazep and dipyridamole. *J Biol Chem* **277**(1):395-401.
- Wang J, Su SF, Dresser MJ, Schaner ME, Washington CB and Giacomini KM (1997) Na⁽⁺⁾-dependent purine nucleoside transporter from human kidney: cloning and functional characterization. *Am J Physiol* **273**(6 Pt 2):F1058-1065.
- Yao SYM, Cass CE and Young JD (2000) Membrane Transport: A Practical Approach, (Baldwin SA ed) pp 47-78, Oxford University Press, Oxford and New York.
- Zhang J, Smith KM, Tackaberry T, Visser F, Robins MJ, Nielsen LP, Nowak I, Karpinski E, Baldwin SA, Young JD and Cass CE (2005) Uridine binding and transportability determinants of human concentrative nucleoside transporters. *Mol Pharmacol* **68**(3):830-839.
- Zhang J, Visser F, Vickers MF, Lang T, Robins MJ, Nielsen LP, Nowak I, Baldwin SA, Young JD and Cass CE (2003) Uridine binding motifs of human concentrative nucleoside transporters 1 and 3 produced in *Saccharomyces cerevisiae*. *Mol Pharmacol* **64**(6):1512-1520.

MOL #48900

FOOTNOTES

This work was supported by research grants from the National Cancer Institute of Canada, the Alberta Cancer Board, and the Canadian Institutes of Health Research. During the course of this work, RJP was supported by the Endowed Graduate Studentship in Oncology: Recruitment Award and a studentship by the Alberta Heritage Foundation for Medical Research. CEC was Canada Research Chair in Oncology and JDY is Heritage Scientist of the Alberta Heritage Foundation for Medical Research.

For reprint requests, contact Dr. Carol E. Cass, Cross Cancer Institute, 11560 University Ave., Edmonton, Alberta, Canada, T6G 1Z2. E-mail: carol.cass@cancerboard.ab.ca

MOL #48900

Legends for figures

Fig. 1. FLT inhibition of ^3H -uridine uptake in yeast cells producing recombinant hNTs. Yeast cells producing a particular recombinant hNT as indicated were incubated with $1\ \mu\text{M}$ ^3H -uridine for up to 30 min in the absence or presence of graded FLT concentrations. Shown are representative experiments performed in quadruplicate and data are expressed as mean \pm SEM. Uptake values represent the percentage of ^3H -uridine uptake in the presence of FLT relative to that in its absence (control). Error bars are not shown where the SEM values were smaller than the size of the symbol.

Fig. 2. (A) Uptake of $20\ \mu\text{M}$ ^3H -thymidine and $20\ \mu\text{M}$ ^3H -FLT in oocytes producing various recombinant hNT proteins. (B) Concentration dependent influx of ^3H -FLT in oocytes producing hNT proteins. Experiments were performed with 12 oocytes per group and data are expressed as mean \pm SEM. Error bars are not shown where the SEM values were smaller than the size of the symbol. Values are for mediated uptake (uptake in RNA transcript-injected oocytes minus uptake in control oocytes injected with water alone).

Fig. 3. Relative quantitation of hNT transcript levels in various cell lines by real-time PCR. hCNT2 transcripts were only detectable in A549 cells. Three to five experiments were performed in triplicate and data are expressed as mean \pm SEM.

Fig. 4. (A) Uptake of $74\ \text{nM}$ ^3H -thymidine and ^3H -FLT in various cell lines in different transport buffers. (B) Mediated uptake of $74\ \text{nM}$ ^3H -FLT in various cell lines in Na^+ buffer with or without $100\ \text{nM}$ NBMPR. Numbers above black columns represent percent uptake inhibited by NBMPR. Three experiments were performed (each in triplicate) and data are expressed as mean \pm SEM.

MOL #48900

Fig. 5. (A) Equilibrium binding of ^3H -NBMPR to MCF-7 cells. Specifically bound ^3H -NBMPR was calculated from the difference between total bound and non-specifically bound (i.e., in the presence of 1 μM non-radioactive NBMPR) (B) Inhibition of 74 nM ^3H -FLT uptake in MCF-7 cells by NBMPR. Only ^3H -FLT uptake inhibited by NBMPR was analyzed in concentration-effect curve. Shown are representative experiments performed in triplicate and data are expressed as mean \pm SEM. Error bars are not shown where the SEM values were smaller than the size of the symbol.

Fig. 6. Equilibrium binding of 10 nM ^3H -NBMPR without (white columns) or with 100 nM FTH-SAENTA (black column) or 10 μM NBMPR (striped column) to various cell lines. Shown is a representative experiment performed in triplicate and data are expressed as mean \pm SEM.

Fig. 7. Linear regression analysis of ^3H -FLT uptake and extracellular NBMPR binding sites per cell for all cell lines excluding MIA PaCa-2. Data in figures were taken from Fig. 4 (FLT uptake in Na^+ buffer) and Table 3. When analyzing all cell lines except MIA PaCa-2, there was a significant correlation between ^3H -FLT uptake and extracellular NBMPR binding sites ($P = 0.0011$, $r^2 = 0.98$).

MOL #48900

TABLES

TABLE 1

Real-time PCR probe and primer concentrations and sequences

Accession			
no. and	Conc.		
oligos	(nM)		Sequence
U81375			
hENT1-F ^a	280		5'-CACCAGCCTCAGGACAGATACAA
hENT1-R	280		5'-GTGAAATACTGAGTGGCCGTCAT
hENT1-P	130		5'-FAM-CCACGGGAGCAGCGTTCCCA
NM_001532			
hENT2-F	280		5'-ATGAGAACGGGATTCCCAGTAG
hENT2-R	280		5'-GCTCTGATTCCGGCTCCTT
hENT2-P	53		5'-FAM-CAGAAAGTAGCTCTGACCCTGGATCTTGACCT
U62968			
hCNT1-F	280		5'-TCTGTGGATTTGCCAATTTTCAG
hCNT1-R	280		5'-CGGAGCACTATCTGGGAGAAGT
hCNT1-P	130		5'-FAM-TGGGAGGCTTGACCTCCATGGTCC
AF036109			
hCNT2-F	900	Purchased as a kit from Applied Biosystems	
hCNT2-R	900	Assay ID Hs00188407_m1	
hCNT2-P	400	(Sequences not given)	
AF305210			
hCNT3-F	280		5'-GGGTCCCTAGGAATCGTGATC
hCNT3-R	280		5'-CGAGGCGATATCACGCTTTC
hCNT3-P	27		5'-FAM-CGGACTCACATCCATGGCTCCTTC
BC001601			

MOL #48900

GAPDH-F	280	5'-GAAGGTGAAGGTCGGAGTC
GAPDH-R	280	5'-GAAGATGGTGATGGGATTTC
GAPDH-P	130	5'-FAM-CAAGCTTCCCGTTCTCAGCC

^a F indicates forward (5') primer; R, reverse (3') primer; P, probe; FAM, 6-carboxyfluorescein.

MOL #48900

TABLE 2

Kinetic parameters of ^3H -FLT influx mediated by hNTs in oocytes

Mean K_m and V_{\max} values (\pm SEM) were determined from the data shown in Figure 2B.

	K_m	V_{\max}	V_{\max}/K_m
hNT	mM	pmol/oocyte/min	ratio
hENT1	3.4 ± 0.2	169 ± 4	50
hENT2	2.6 ± 0.4	180 ± 13	69
hCNT1	0.13 ± 0.01	52 ± 1	400
hCNT3	0.11 ± 0.01	37 ± 1	340

MOL #48900

TABLE 3

NBMPR binding parameters and IC₅₀ values for inhibition of ³H-FLT uptake in various cell lines

Experiments were performed at least three times (each experiment in triplicate) and data are expressed as mean ± SEM.

Cell Line	NBMPR				Extracellular NBMPR	
	IC ₅₀ (nM)	K _d (nM)	B _{max} (fmol/10 ⁶ cells)	Binding (10 ⁵ sites/cell)	%	Binding 10 ⁵ sites/cell
MCF-7	0.21 ± 0.01	0.23 ± 0.04	450 ± 76	2.7 ± 0.5	71 ± 9	1.9 ± 0.3
A549	0.22 ± 0.13	0.26 ± 0.07	360 ± 18	2.2 ± 0.1	60 ± 7	1.3 ± 0.06
U251	0.93 ± 0.28	0.20 ± 0.03	340 ± 33	2.0 ± 0.2	47 ± 5	1.0 ± 0.09
A498	0.31 ± 0.07	0.18 ± 0.02	270 ± 25	1.6 ± 0.2	38 ± 4	0.6 ± 0.06
MIA PaCa-2	1.15 ± 0.11	0.38 ± 0.05	1300 ± 210	7.9 ± 1.3	56 ± 3	4.4 ± 0.7
Capan-2	0.21 ± 0.04	0.43 ± 0.05	180 ± 25	1.1 ± 0.2	1.6 ± 1.6	0.02 ± 0.002

Figure 1

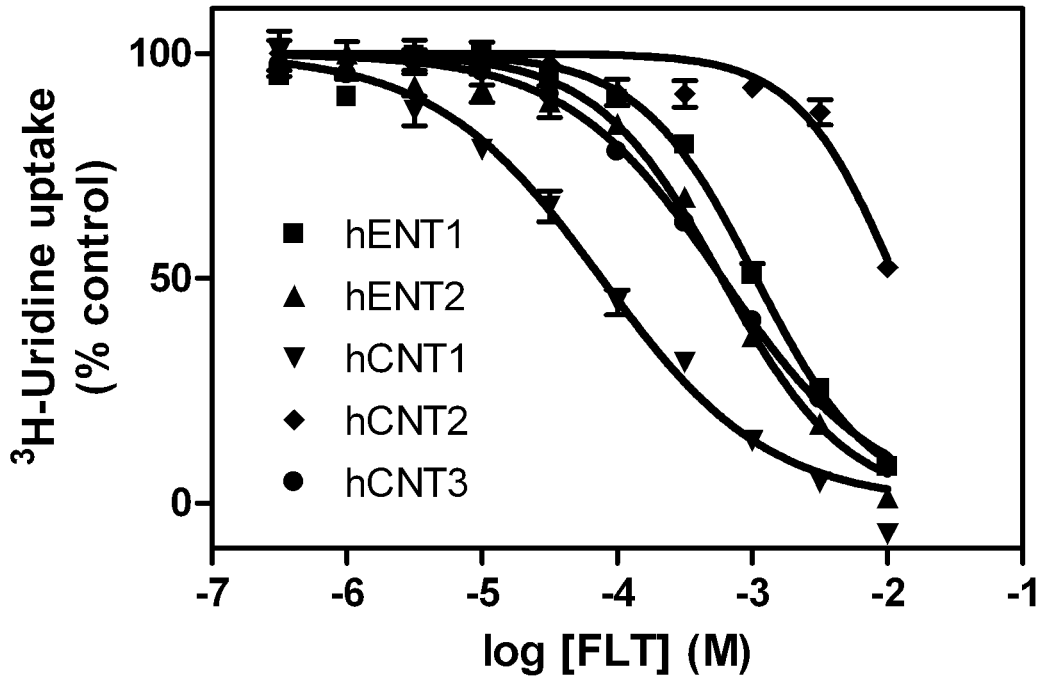


Figure 2

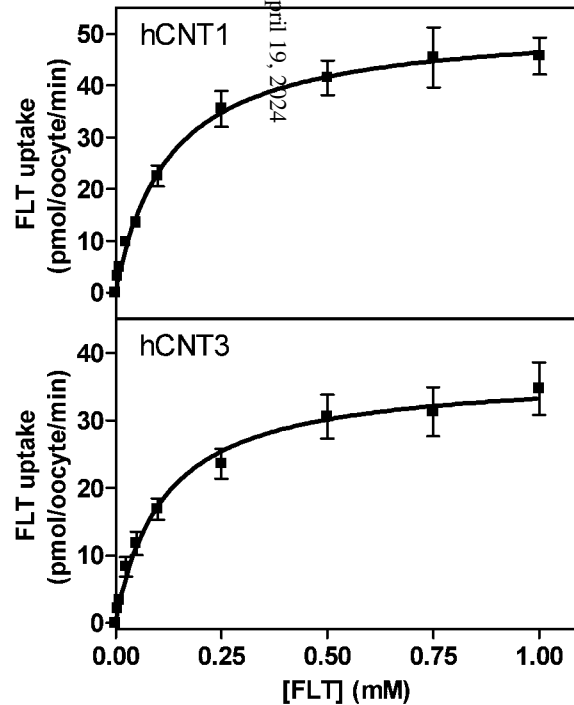
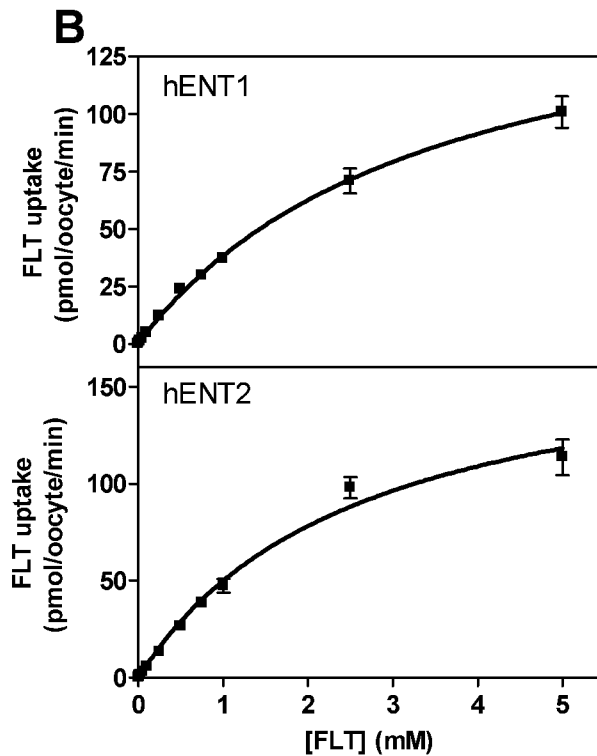
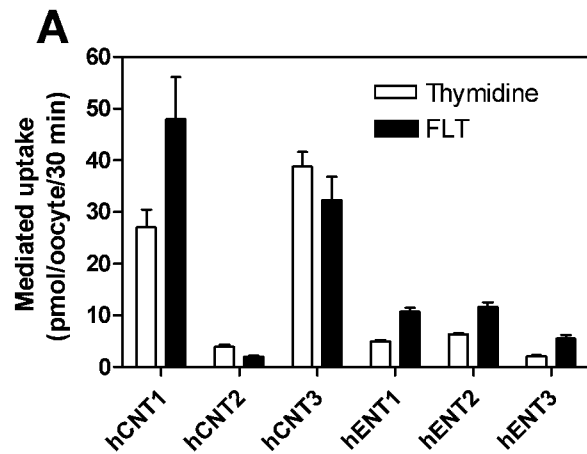


Figure 3

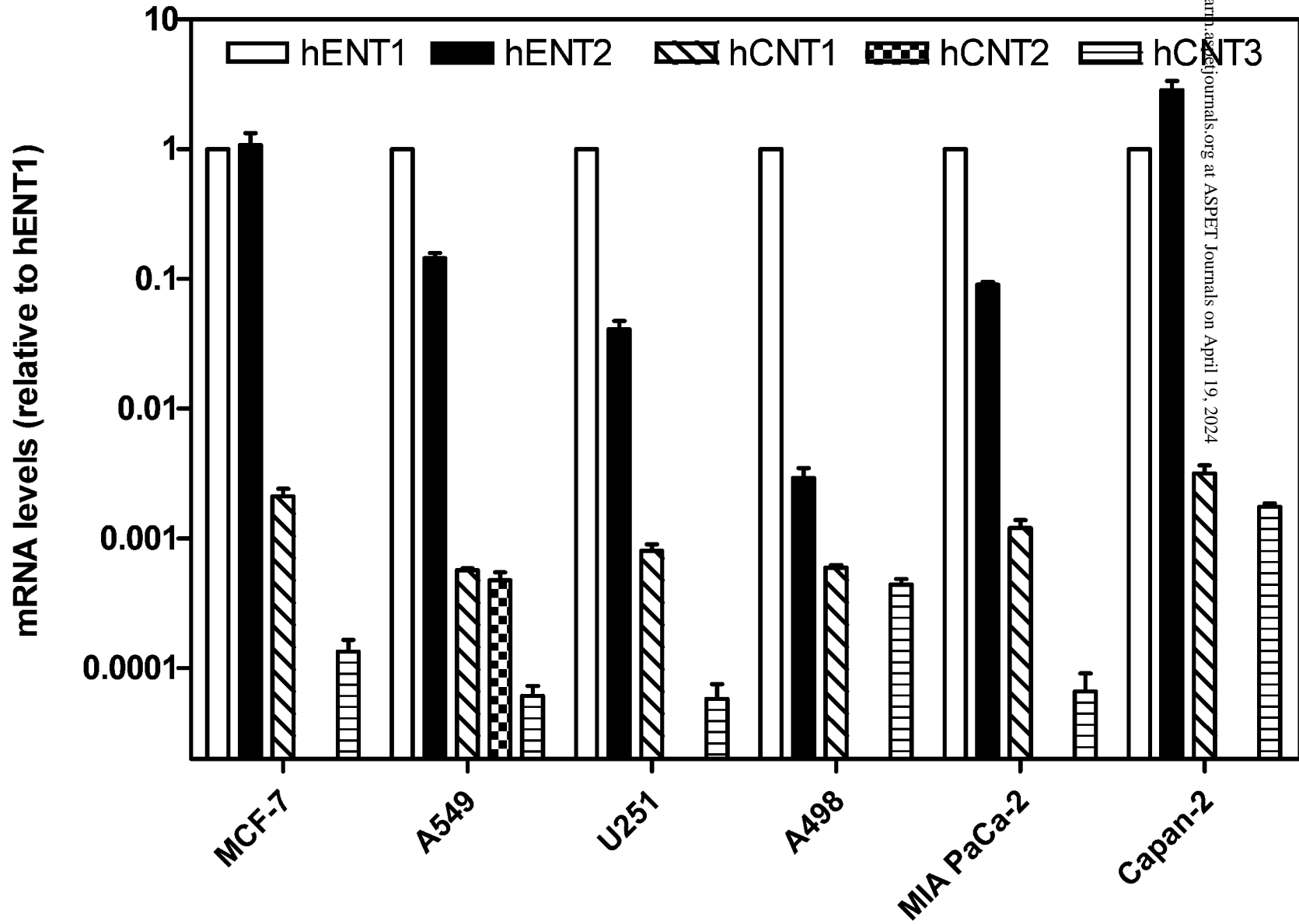


Figure 4

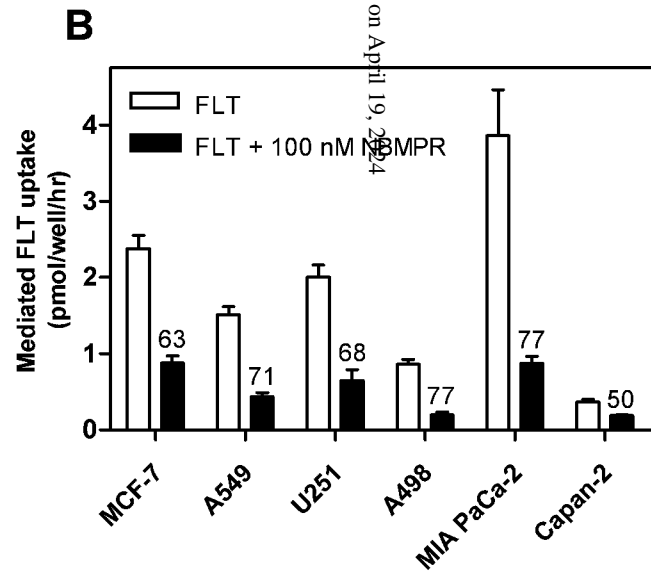
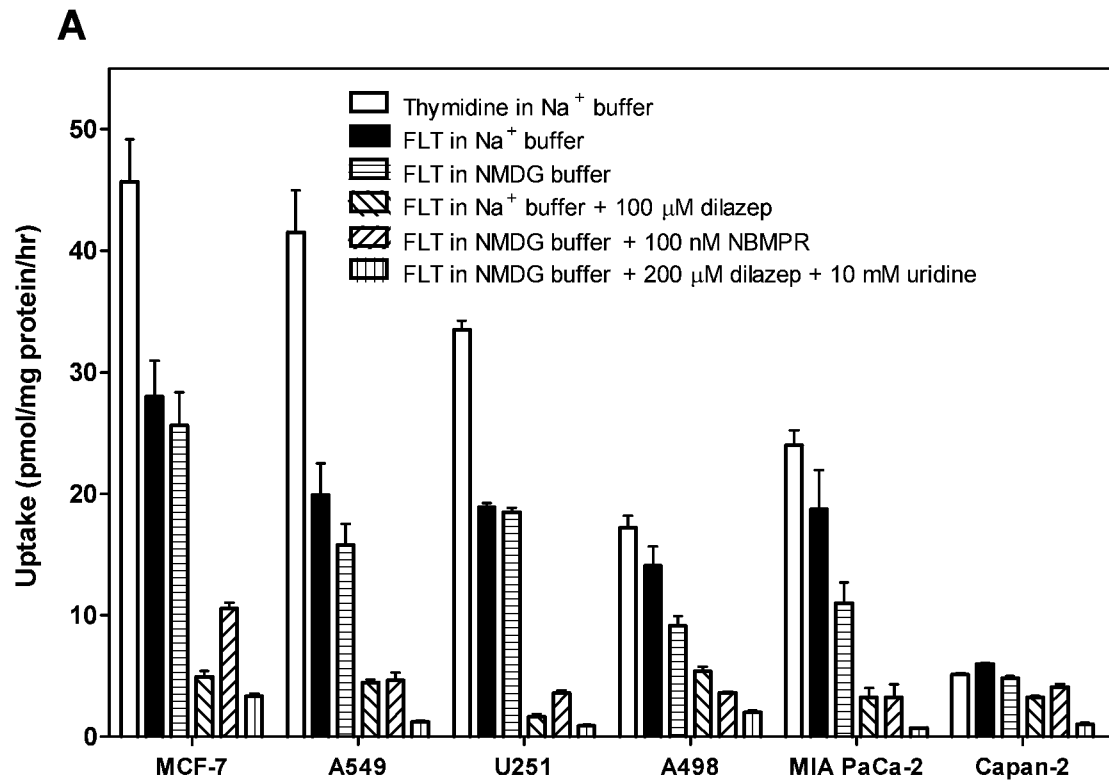
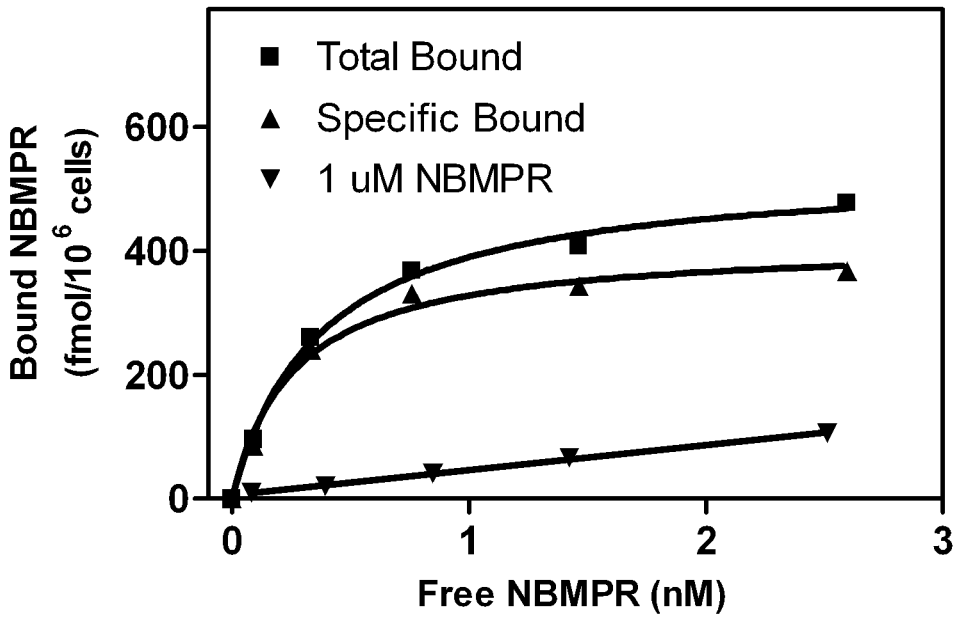


Figure 5

A



B

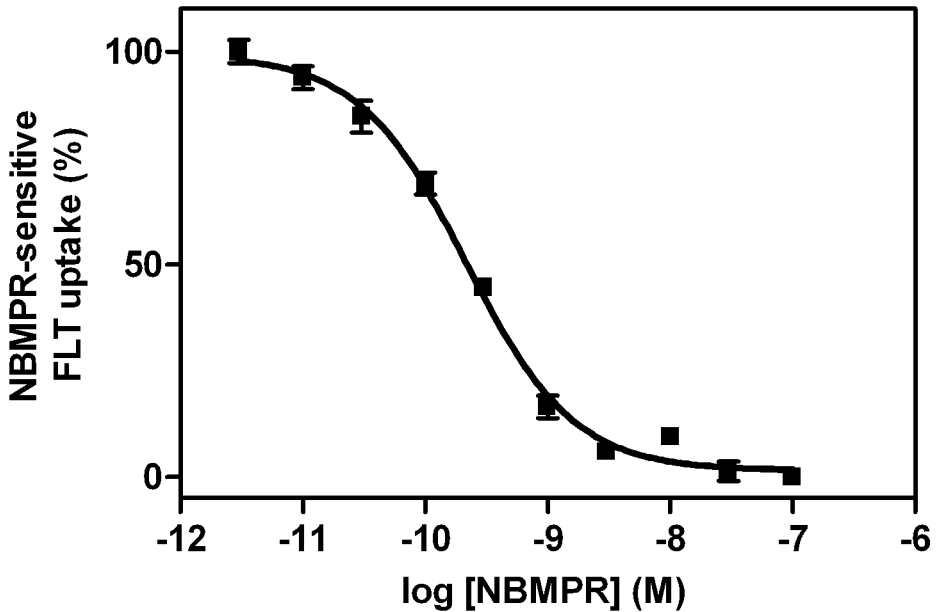


Figure 6

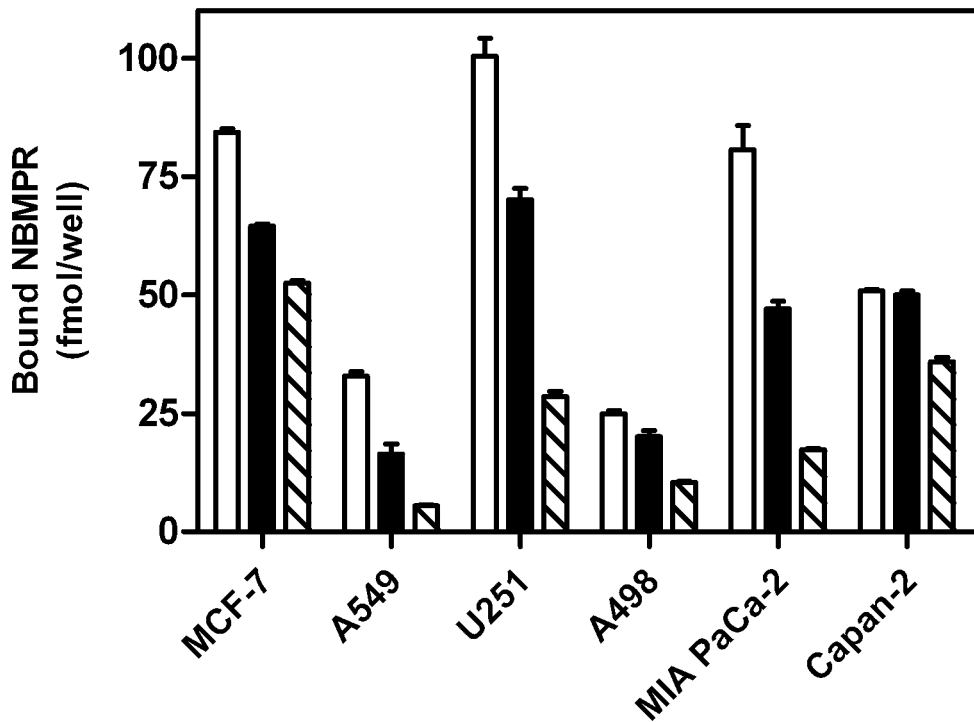


Figure 7

